Effects of TiO_2 Surface Fluorination on Photocatalytic Reactions and Photoelectrochemical Behaviors

Hyunwoong Park and Wonyong Choi*

School of Environmental Science and Engineering and Department of Chemistry, Pohang University of Science and Technology, Pohang, Korea 790-784

Received: September 14, 2003; In Final Form: January 5, 2004

The formation of surface fluorides on TiO_2 ($F-TiO_2$), which can be easily attained by a simple addition of F^- to aqueous TiO_2 suspensions, uniquely affects both photocatalytic reactions and photoelectrochemical behaviors. The fluoride adsorption is favored at acidic pH and greatly reduces the positive surface charge on TiO_2 by replacing $\equiv Ti-OH_2^+$ by $\equiv Ti-F$ species. Effects of surface fluorination on the photocatalytic reactivities are very different depending on the kind of substrates to be degraded. $F-TiO_2$ is more effective than pure TiO_2 for the photocatalytic oxidation of Acid Orange 7 and phenol, but less effective for the degradation of dichloroacetate. It is proposed that the OH radical mediated oxidation pathways are enhanced on $F-TiO_2$, whereas the hole transfer mediated oxidations are largely inhibited due to the hindered adsorption (or complexation) of substrates on $F-TiO_2$. As for the photocatalytic reduction, the dechlorination of trichloroacetate is much reduced on $F-TiO_2$. The photocurrents collected in TiO_2 suspensions, which are mediated by electron shuttles (methyl viologen or ferric ions), and short-circuit photocurrents generated on an illuminated TiO_2/Ti electrode are also markedly reduced in the presence of F^-. The surface $\equiv Ti-F$ group seems to act as an electron-trapping site and to reduce interfacial electron transfer rates by tightly holding trapped electrons due to the strong electronegativity of the fluorine. Finally, elementary charge transfer processes on $F-TiO_2$ and their implications to photocatalytic reaction pathway are discussed.

Introduction

Semiconductor photocatalysis has been intensively investigated for its application to environmental pollutants degradation.[1−5] Since heterogeneous photocatalytic reactions take place on the surface, the surface properties of the semiconductor play a critical role in determining photocatalytic reaction efficiencies and mechanisms. Surface properties of TiO_2, the most popular semiconductor photocatalyst, are related with various parameters such as pH, surface hydroxyl groups, particle size, crystalline phase, surface defects, surface metal deposits, and adsorbates or surface complexes. TiO_2 surfaces have been actively modified through manipulating the above parameters in order to optimize or control the photocatalytic reactions.[1,5f−h,6]

Fluorinated TiO_2 has been often investigated in relation to doping ($TiO_{2-x}F_x$)[7−12] or surface complexation ($F-TiO_2$).[11−15] It was reported that fluoride doping improves the crystallinity of anatase and the photocatalytic reactivity.[8−10] In addition, $TiO_{2-x}F_x$ has fewer anion vacancies with a lower density of midgap states,[7−9,12] and is more stable against photocorrosion.[11] On the other hand, surface fluorination of TiO_2 ($F-TiO_2$) is a simple ligand exchange between fluoride anions (F^-) and surface hydroxyl groups on TiO_2 in water (reaction 1).[13,14] [The notation "$\equiv Ti-X$" represents surface species throughout the text.]

$$\equiv Ti-OH + F^- \leftrightarrow \equiv Ti-F + OH^- \qquad pK_F = 6.2 \text{ (ref 16)} \tag{1}$$

The extent of fluorination on TiO_2 highly depends on pH, showing a maximum (~99%) around pH 3−4. It was recently reported that the surface fluorination of TiO_2 improves the photocatalytic oxidation rate of phenol[13] and tetramethylammonium (TMA^+)[14] at a specific pH range. Since the surface fluorides themselves should not be reactive with valence band (VB) holes [$E°(F^•/F^-) = 3.6$ V vs NHE],[15,17] the higher photocatalytic oxidation rate in the $F-TiO_2$ suspension has been ascribed to the enhanced generation of mobile free OH radicals (reaction 2) whereas most OH radicals generated on naked TiO_2 surface prefer to remain adsorbed (reaction 3).[13]

$$\equiv Ti-F + H_2O \text{ (or } OH^-) + h_{vb}^+ \rightarrow \equiv Ti-F + {}^•OH_{free} + H^+ \tag{2}$$

$$\equiv Ti-OH + h_{vb}^+ \rightarrow \equiv Ti-OH^{•+} \tag{3}$$

This implies that the photocatalytic reactions in the $F-TiO_2$ suspension could be initiated in the solution bulk remote from the TiO_2 surface. However, the surface fluoride enhanced effect was not observed in the gas-phase photocatalytic reactions.[15]

Although the surface fluoride effects on photocatalytic reactions have been undoubtedly recognized, understanding of reaction mechanisms operating at the $F-TiO_2$/water interface is still not clear. First of all, the surface fluorination of TiO_2 should affect not only the VB hole transfer (hence the OH radical formation) but also the conduction band (CB) electron transfer since electron and hole transfers on a TiO_2 particle are closely related in order to maintain an electroneutrality condition. Most photocatalytic reactions taking place on the TiO_2 surface consist of a series of electron and hole transfers. In addition, the surface adsorption or complexation of initial substrates (or intermediates) on the TiO_2 surface should be affected, which

* Corresponding author. E-mail: wchoi@postech.ac.kr.

10.1021/jp036735i CCC: $27.50
Published on Web 03/09/2004

consequently modifies the reaction kinetics and mechanisms. Therefore, the overall effects of surface fluorination on photocatalytic reactions should be complex.

In this study, we investigated the effects of surface fluorides on TiO_2 on both photocatalytic reactions of four organic compounds whose degradation mechanisms are quite different from one another and the photocurrent generation behaviors. The results show that the surface fluorination of TiO_2 clearly enhances the OH radical mediated degradation but inhibits the hole transfer mediated path on the contrary because the substrate adsorption or complexation is prohibited on F−TiO_2. The surface ≡Ti−F group seems to serve as an electron-trapping site but reduces interfacial electron transfer rates by tightly holding trapped electrons. As a result, both photoreductive reaction rate and photocurrent generation are reduced on F−TiO_2.

Experimental Section

Materials and Reagents. TiO_2 powder (Degussa P25), a mixture of anatase and rutile (8:2), was used as received as a photocatalyst. This commercial TiO_2 was selected in this study for its wide popularity as a photocatalyst and because there is plenty of published data on its photocatalytic behaviors. Sodium fluoride (NaF) was added to aqueous TiO_2 suspensions to fluorinate the TiO_2 surface. The effect of chlorides was investigated by adding NaCl instead. 4-(2-Hydroxy-1-naphthylazo)benzenesulfonic acid (Acid Orange 7, AO7) (85%, Aldrich), phenol (99%, Junesi), sodium dichloroacetate (DCA) (98%, Aldrich), sodium trichloroacetate (TCA) (97%, Aldrich), methanol (Aldrich), and *tert*-butyl alcohol (Shinyo) were used as substrates or reagents in photocatalytic reactions. A platinum plate (1 × 1 cm^2, 0.125 mm thick, 99.9%, Aldrich), a Ti plate (2.5 × 2.5 cm^2, 0.5 mm thick, 99.99%, Aldrich), methyl viologen (MV^{2+}) dichloride hydrate (98%, Aldrich), sodium acetate (Merck), and $FeCl_3 \cdot 6H_2O$ (>99%, Kanto) were used in photoelectrochemical experiments. Platinized TiO_2 (Pt/TiO_2) with a typical Pt loading of 0.2 wt % was prepared using a photodeposition method and H_2PtCl_6 as a precursor as described previously.[18] NaOH, HCl, and $HClO_4$ were used for the pH adjustment of aqueous suspensions.

Photocatalytic Reactivity Test. An 80-mL glass reactor with a quartz window was used in photocatalytic reaction experiments. Substrate (AO7, phenol, DCA, or TCA), NaF, and other necessary reagents were added to an aqueous TiO_2 suspension in the reactor and equilibrated for 30 min prior to illumination. A 300-W Xe arc lamp (Oriel) was used as a light source. Light passed through a 10-cm IR water filter and a cutoff filter (λ > 300 nm for UV or λ > 420 nm for visible light illumination), and then the filtered light was focused onto the reactor. When a deaerated condition was required, N_2 gas (> 99.9%) was continuously purged through the suspension. Sample aliquots were withdrawn by a 1-mL syringe intermittently during the illumination and filtered through a 0.45-μm PTFE filter (Millipore).

The degradation of AO7 was monitored by measuring the absorbance at λ = 485 nm as a function of irradiation time with a UV−vis spectrophotometer (Shimadzu UVPC-2401). Phenol and its degradation intermediates were analyzed with a reverse-phase high performance liquid chromatograph (HPLC, Agilent 1100 series). The eluent solution was composed of acetonitrile (20%) and phosphoric acid−added water (80%). For the analysis of DCA, TCA, and Cl^-, an ion chromatograph (IC, Dionex DX-120) that was equipped with a Dionex IonPac AS 14 (4 mm × 250 mm) column and a conductivity detector was employed. The eluent solution was 3.5 mM Na_2CO_3/1 mM $NaHCO_3$.

Photoelectrochemical Experiments. Measurements of photocurrent collected on an inert electrode (Pt) immersed in aqueous suspensions of TiO_2, F−TiO_2, or Pt/TiO_2 were carried out as described in our recent paper.[18] In a 100-mL glass reactor with a Pyrex window (5 cm in diameter) for UV illumination, TiO_2 (or Pt/TiO_2), NaF, acetate (electron donor), and MV^{2+} or Fe^{3+} (reversible electron shuttle) were added in distilled water, and the suspension pH was adjusted with $HClO_4$ or NaOH. A platinum plate (1 × 1 cm^2), a saturated calomel electrode (SCE), and a graphite rod were immersed in the reactor as working (collector), reference, and counter electrodes, respectively. Nitrogen gas was continuously purged though the suspension. Photocurrents were collected in the suspension by applying a potential (+0.6 V vs SCE) to the Pt working electrode using a potentiostat (EG&G 263A2) connected to a computer. A 30-W black light lamp (ca. 130 μW/cm^2 for 300 < λ < 400 nm) was a UV light source. The suspension was magnetically stirred throughout the photocurrent measurements.

Photocurrent generation was also measured with a TiO_2 electrode (naked vs fluorinated) immersed in aqueous solution. For the preparation of TiO_2 electrode, a titanium plate (2.5 × 2.5 cm^2) was washed with detergent, immersed in a 5% HF solution for 5 min, subsequently immersed in an acidic mixture (3 mL of 50% HF + 3 mL of 70% HNO_3 + 3 mL of 30% H_2O_2) for 1 min, washed with distilled water and dried, and then oxidized at 500 °C for 1 h. The resulting TiO_2/Ti electrode, an SCE, and Pt gauze were used as working, reference, and counter electrodes, respectively, in the photocurrent measurement. The 30-W black light lamp was employed as a light source.

Surface Characterization. For the surface analysis of F−TiO_2, TiO_2 suspension (1 g/L) with 10 mM NaF at a specific pH was filtered through a 0.45 μm filter, dried at 95 °C overnight, and pelletized to thin disks with a high-pressure pelletizer (Carver). These pellets were analyzed with X-ray photoelectron spectroscopy (XPS, Kratos XSAM 800 pci) using Mg Kα lines (1253.6 eV) as an excitation source. The spectra were taken for each sample after Ar^+ (3 keV) sputter cleaning. Surface charging was minimized by spraying low energy electrons over the sample surface using a neutralizer gun. Binding energy spectra were recorded in the regions of C 1s, Ti 2p, O 1s, and F 1s. The binding energies of all peaks were referenced to the C 1s line (284.6 eV) originating from surface impurity carbons.

The optical absorption spectra of pure TiO_2 and F−TiO_2 powder were recorded with a UV−vis spectrophotometer equipped with a diffuse reflectance attachment (Shimadzu ISR-2200). All sample powders were diluted with $BaSO_4$ (TiO_2:$BaSO_4$ = 1:17) and referenced to $BaSO_4$.

The electrophoretic mobilities of TiO_2 particles in aqueous suspensions were measured to determine their zeta potentials as a function of pH and [F^-] using an electrophoretic light scattering spectrophotometer (ELS 8000, Otsuka) equipped with a He−Ne laser and a thermostated flat board cell.

Results and Discussion

Characterization of F−TiO_2 Surface. Figure 1 shows the XPS survey spectrum of fluorinated TiO_2 powder that was prepared by adding NaF in the aqueous TiO_2 suspension at pH 3.6, filtering, and drying. The F−TiO_2 sample clearly shows the peak of F 1s as well as those of Ti, O, and C elements. The F 1s peak is originated from the surface fluoride (≡Ti−F) formed by ligand exchange between F^- and surface hydroxyl group on TiO_2. The F 1s binding energy (BE) of 684.3 eV in

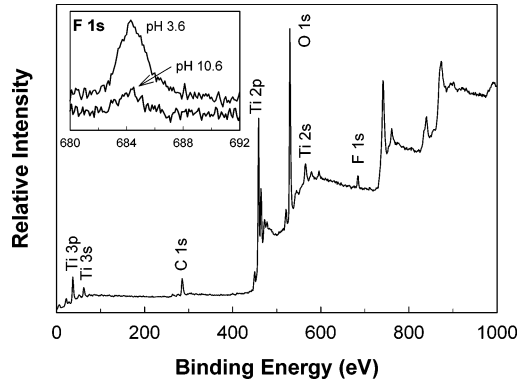

Figure 1. XPS survey spectrum of fluorinated TiO_2 ($F-TiO_2$) powder prepared at pH 3.6. The inset compares the F 1s peak intensity of $F-TiO_2$ samples prepared at pH 3.6 and 10.6.

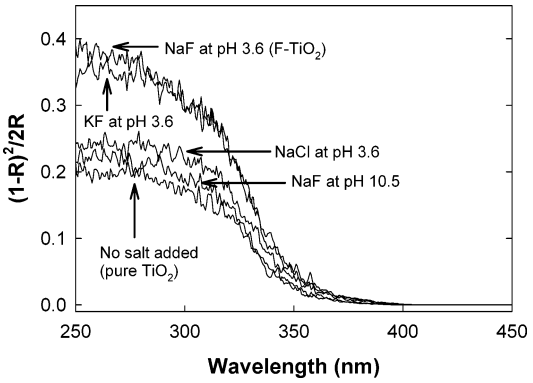

Figure 2. UV−vis diffuse reflectance spectra of naked TiO_2 and $F-TiO_2$ powders prepared at pH 3.6 and 10.5. All powder samples were prepared from the aqueous suspensions containing the indicated salts through filtering and subsequent drying. TiO_2 samples were diluted with $BaSO_4$ (1:17). The ordinate scale is expressed in the Kubelka−Munk unit.

this spectrum (inset of Figure 1) corresponds to that of F^- adsorbed on TiO_2, and no sign of F ions in the lattice (BE = 688.5 eV) was found.[10] The surface fluorination of TiO_2 hardly takes place at pH 10.6, which indicates that the fluoride adsorption is greatly reduced at alkaline pH.[14] Figure 2 compares the UV diffuse reflectance spectra of TiO_2 powder samples that were prepared from the aqueous suspensions containing NaF, KF, or NaCl through filtering and drying. The UV absorption (expressed in the Kubelka−Munk unit) of $F-TiO_2$ prepared at pH 3.6 is higher than that of pure TiO_2 at $\lambda < 400$ nm, whereas the absorption edge region is unaffected by the surface fluorination. The absorption spectrum of NaCl-treated TiO_2 powder shows little difference from that of pure TiO_2. The absorption spectrum of KF-treated TiO_2 is almost identical to that of NaF-treated TiO_2, which indicates that a cation effect on UV absorption is absent. $F-TiO_2$ prepared at pH 10.5, which has an insignificant concentration of surface fluorides (inset of Figure 1), exhibits a UV absorption spectrum that is little different from that of pure TiO_2, which suggests that surface fluoride species are responsible for higher UV absorption. Another interesting observation is that the as-received TiO_2 powder (P25) shows higher UV absorption (or lower reflectance) than the same powder that was obtained from an aqueous suspension in pure distilled water through filtering and drying (data not shown). This seems to imply that increasing water adsorption on TiO_2 increases the UV reflectivity of the powder. On the contrary, the fluoride adsorption on TiO_2 decreases the UV reflectivity. These observations suggest that the UV reflectivity of TiO_2 powder seems to be closely related to the surface properties. Further studies are needed to address this issue. It was also observed by Yu et al.[10] that F-doped TiO_2 ($TiO_{2-x}F_x$) exhibits higher UV absorbance and a red shift in the band gap compared with pure TiO_2, although the reason was not clear. However, the present surface fluorinated TiO_2 ($F-TiO_2$) shows no change in the absorption edge. X-ray diffraction (XRD) patterns of TiO_2 and $F-TiO_2$ powder samples showed no difference, which indicates that surface fluorination at ambient temperature does not affect the crystallinity at all.

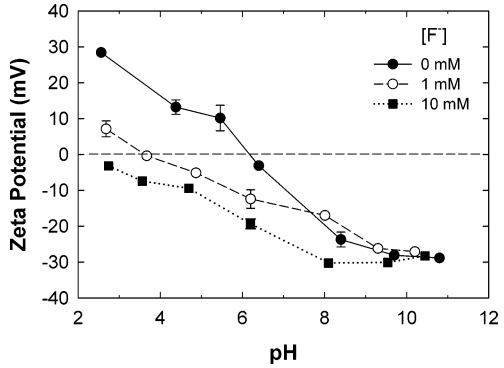

Figure 3. Zeta potentials of TiO_2 particles in aqueous suspensions ($[TiO_2] = 2$ mg/L) as a function of pH and $[F^-]$.

Figure 3 shows the variation of zeta potentials of suspended TiO_2 particles in water as a function of pH and $[F^-]$. The point of zero zeta potential (PZZP) of TiO_2 is measured to be ca. pH 6.2, which is in agreement with the literature value.[19−21] In the presence of F^-, the PZZP is shifted to lower pH values and the positive charge on TiO_2 surface at acidic pH region is much reduced since the surface $\equiv Ti-OH_2^+$ groups are replaced by $\equiv Ti-F$ species. As a result, the concentration of TMA^+ at the TiO_2/water interface (at pH 3) was higher on $F-TiO_2$ than on naked TiO_2 film due to a reduced electrostatic repulsion between the cation and the surface.[14] In general, the complexation between surface Ti(IV) sites and ligands should affect the surface charge density and consequently the zeta potentials. In addition, it is interesting to note that the measured TiO_2 zeta potential is negative in most of the pH range in the presence of F^-. This is somewhat different from the previously calculated[14] surface charge distribution, which shows that the TiO_2 surface charge is near zero in the range pH 3−7 even in the presence of 5−20 mM F^-. The discrepancy is largely due to the physical adsorption of F^- on TiO_2, which was not taken into account when modeling the surface charge of TiO_2.

Photocatalytic Reactivity of $F-TiO_2$. It has been recently reported that the surface fluorination of TiO_2 enhanced the photocatalytic oxidation rate of phenol[13] and TMA^+.[14] To investigate the effects of the surface fluoride on photocatalytic redox reactions, four model compounds whose photocatalytic degradation mechanisms are quite different from one another were selected as target substrates in this study: AO7, phenol, dichloroacetic acid (DCA), and trichloroacetic acid (TCA).

Figure 4a shows the adsorption isotherms of AO7 on TiO_2 or $F-TiO_2$ at pH 4. In the absence of NaF, AO7 is significantly adsorbed on TiO_2 surface (ca. 30% of AO7 adsorbed at $[AO7]_i = 100$ μM) mainly because of the electrostatic attraction between anionic AO7 and positively charged TiO_2 surface ($\equiv Ti-OH_2^+$). In contrast, in the presence of NaF, AO7 adsorption on TiO_2 is almost completely inhibited. At pH 4 and $[F^-] = 10$ mM, ca. 95% of surface hydroxyl groups of TiO_2 are calculated to be replaced with chemisorbed F^- ($\equiv Ti-F$).[14] As a result, the surface charge is near zero or even reversed to negative with excess fluorides due to the presence of physisorbed

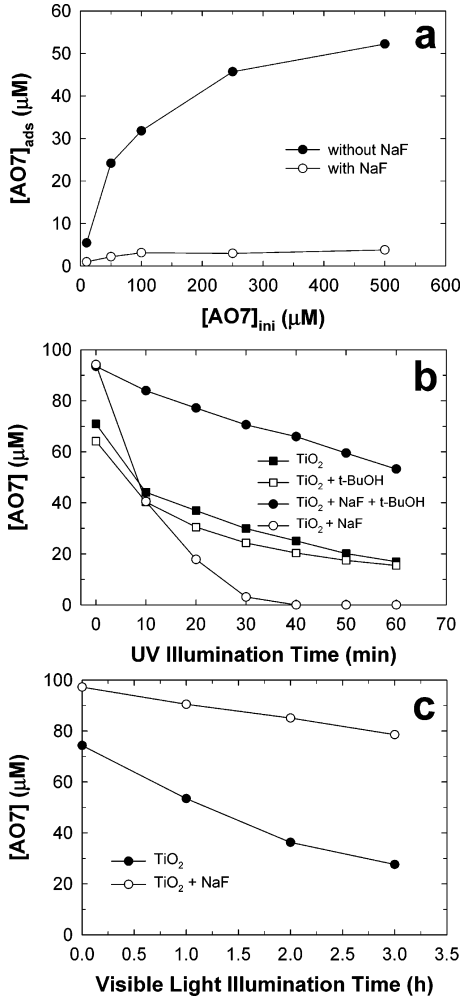

Figure 4. (a) Dark adsorption isotherm of AO7 in aqueous TiO_2 suspension at pH 4 with or without NaF. (b) UV (λ > 300 nm) induced degradation of AO7 in TiO_2 suspension with or without NaF and *t*-BuOH. (c) Visible light (λ > 420 nm) induced degradation of AO7 in TiO_2 suspension with or without NaF. Experimental conditions: $[TiO_2] = 0.5$ g/L; $[AO7]_0 = 100$ μM (except for part a); [NaF] = 10 mM; [*t*-BuOH] = 0.1 M (added in the indicated case only); $pH_i = 4.0$; open to air.

F^- (Figure 3), which should repel AO7 anions electrostatically with a drastic reduction in AO7 adsorption. The change of surface property should directly affect the photocatalytic reactivity.

Figure 4b compares photocatalytic degradation of AO7 in TiO_2 and F−TiO_2 suspensions. Despite little adsorption of AO7 on F−TiO_2, the photocatalytic degradation rate of AO7 in the F−TiO_2 suspension is much enhanced from that in the pure TiO_2 suspension. This concurs with the result of Minero et al.[13a] that catechol degraded faster on F−TiO_2 than on naked TiO_2 despite its hindered adsorption on F−TiO_2. These observations imply two facts. First, the photocatalytic degradation of substrates in the F−TiO_2 suspension could be initiated in the solution bulk (not on the surface) probably through the action of mobile oxidants (reaction 2).[5d,13a,14] Second, the overall efficiency of photocatalytic degradation of aromatic substrates on TiO_2 could be limited by the role of the aromatic moiety as a charge recombination center.[13a,22] As a result, the reduced adsorption of aromatic compounds could enhance their photocatalytic degradation rate provided that mobile oxidants are available in the solution bulk. In addition, adding *tert*-butyl alcohol (*t*-BuOH) as a hydroxyl radical scavenger induces very different responses between the pure TiO_2 and F−TiO_2 systems.

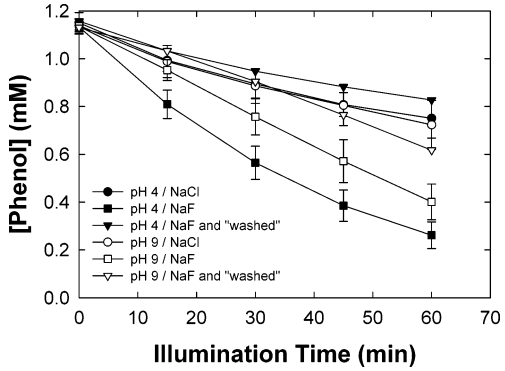

Figure 5. Time profiles of photodegradation of phenol in UV-illuminated TiO_2 suspension with NaF or NaCl at pH 4 and 9. "Washed" refers to washing out the filtered powders with distilled water until no detection of fluoride anion. Experimental conditions: $[TiO_2] = 0.5$ g/L; $[phenol]_0 = 1.14$ mM; [NaCl] = [NaF] = 10 mM; open to air.

The addition of *t*-BuOH greatly reduces the photodegradation rate of AO7 in the F−TiO_2 suspension, whereas its addition has little effect on the AO7 degradation in the pure TiO_2 suspension. This implies that the AO7 photodegradation in the F−TiO_2 suspension proceeds through a mechanistic path that is different from that on naked TiO_2. AO7 degradation on naked TiO_2 seems to be initiated mostly by the direct hole transfer, whereas OH radicals play the role of a main oxidant in the F−TiO_2 system. This case is quite different from the previously reported effect of *t*-BuOH on phenol,[13b] which showed that the phenol photodegradation rates were markedly reduced in the presence of *t*-BuOH for both naked TiO_2 and F−TiO_2. From the detailed kinetic analysis of the effect of alcohols, Minero et al.[13b] suggested that the phenol photodegradation on naked TiO_2 is largely mediated by surface OH radicals whereas that on F−TiO_2 is almost entirely ascribed to homogeneous OH radicals. That is, on naked TiO_2, the photocatalytic degradation of phenol and AO7 is mainly mediated by surface OH radicals and VB holes, respectively. On F−TiO_2, however, both phenol and AO7 are degraded largely through the action of OH radicals.

Figure 4c compares the visible light (λ > 420 nm) sensitized degradation of AO7 in the TiO_2 and F−TiO_2 suspensions. Photosensitized degradation of organic dyes (or colored substances) on visible light illuminated TiO_2 has been frequently studied.[23−25] This process is known to be initiated by a direct electron transfer from a photoexcited dye molecule to TiO_2 CB. Since OH radicals cannot be generated under visible light, visible light induced degradation of dyes requires that dye molecules be in direct contact with the TiO_2 surface for an efficient electron injection. In accordance with this expectation, the visible light induced degradation of AO7 on F−TiO_2 where AO7 adsorption is inhibited is markedly reduced.

Figure 5 compares the time profiles of photocatalytic degradation of phenol in the naked TiO_2 (TiO_2 + NaCl) and F−TiO_2 (TiO_2 + NaF) suspension at pH 4 and 9. The photodegradation rate of phenol in the F−TiO_2 suspension at pH 4 is ca. 2.5 times as fast as that in the naked TiO_2 suspension, which reconfirms the result of Minero et al.[13a] The situation should be very similar to the case of AO7. However, it has not been recognized in the previous study that the fluoride-enhancement effect is observed even at pH 9, where the surface concentration of ≡Ti−F species should be negligible.[14] This behavior cannot be understood in terms of the equilibrium surface speciation on TiO_2. A plausible explanation is proposed later. The reactivities of F−TiO_2 powder samples that were washed with distilled water and then resuspended were similar

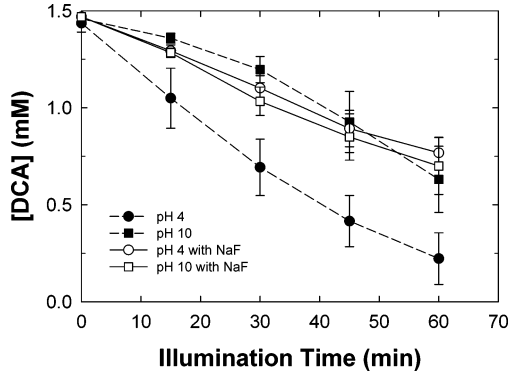

Figure 6. Comparison of photodegradation time profiles of dichloroacetate (DCA) in UV-illuminated TiO_2 suspensions with or without NaF at pH 4 and 10. Experimental conditions: $[TiO_2] = 0.1$ g/L; $[DCA]_0 = 1.47$ mM; $[NaF] = 1$ mM; open to air.

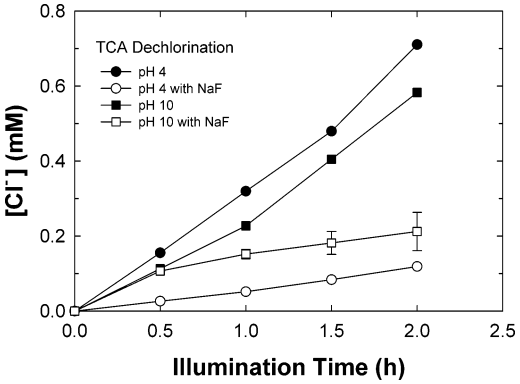

Figure 7. Comparison of photoreductive dechlorination of trichloroacetate (TCA) in deaerated and UV-illuminated TiO_2 suspensions with or without NaF at pH 4 and 10. Methanol was added as an electron donor. Experimental conditions: $[TiO_2] = 0.1$ g/L; $[NaF] = 1$ mM; $[TCA]_0 = 5$ mM; $[MeOH] = 0.24$ M; continuously N_2-purged.

to those of pure TiO_2. This clearly indicates that fluoride anions do not irreversibly adsorb on TiO_2 surface.

Figure 6 shows the photocatalytic degradation profiles of dichloroacetate (DCA) in the F−TiO_2 and naked TiO_2 suspensions at pH 4 and 10. In contrast to the cases of AO7 and phenol, the photodegradation rate of DCA markedly decreases in the presence of F^- at pH 4. It was proposed that the photocatalytic degradation of DCA on TiO_2 is mainly initiated by a direct hole transfer through the formation of bidentate complexes at acidic pH, and thus DCA adsorption on TiO_2 surface is the rate-liming step in its photodegradation.[26] Since replacing ≡Ti−OH by ≡Ti−F should inhibit the DCA complexation at the surface and consequently make the direct hole transfer unfavorable, DCA photodegradation rate is reduced on F−TiO_2. Although DCA can be attacked by surface-bound or free OH radicals as well, its reaction with VB holes seems to be faster. At pH 10 where the surface fluorination is negligible, the fluoride addition has little effects on the photodegradation rate of DCA.

Figure 7 compares the time profiles of chloride production from the photocatalytic degradation of trichloroacetate (TCA) in the pure TiO_2 and F−TiO_2 suspensions at pH 4 and 10. TCA is known to be degraded via a reductive pathway (reaction 4).[27]

$$CCl_3CO_2^- + e_{cb}^- \rightarrow {}^{\bullet}CCl_2CO_2^- + Cl^- \qquad (4)$$

The dechlorination rates are greatly reduced in the F−TiO_2 suspension at pH 4, which could be ascribed to two reasons. First, the TCA adsorption (or complexation) on F−TiO_2 should be reduced as in the case of DCA. Second, we may assume

SCHEME 1 [a]

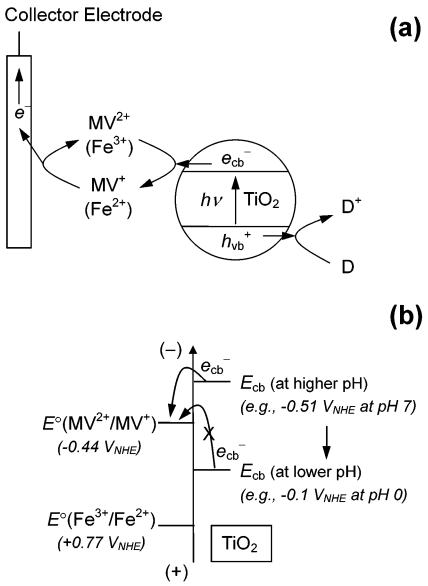

(a) Methyl viologen (MV^{2+}) mediated (or Fe^{3+} mediated) current collection on an inert Pt electrode immersed in UV-illuminated TiO_2 suspension. D represents an electron donor, which is acetate in this study. (b) Comparison of energetics of pH-dependent TiO_2 CB and pH-independent MV^{2+} (or Fe^{3+}) reduction potential.

that the rate of CB electron transfer to TCA on F−TiO_2 is intrinsically slower. At pH 10 where the fluoride adsorption on TiO_2 is negligible and the zeta potential of TiO_2 is unaffected by the presence of F^- (see Figure 3), the chloride production rate in the initial period (<30 min) is not affected by the presence of F^-, but is significantly reduced in the later illumination period. The fluoride effect in the alkaline pH was also observed in the case of phenol photodegradation (see Figure 5): the differences in the residual phenol concentration between the NaCl/pH 9 and NaF/pH 9 systems get progressively larger with increasing illumination time. It seems that the fluoride adsorption on TiO_2 takes place slowly even at alkaline condition under illumination.

Photoelectrochemical Investigations. The assumption that CB electron transfer kinetics could be intrinsically slower on F−TiO_2 than on naked TiO_2 needs more evidence. To investigate how CB electron transfer behaviors on TiO_2 particles are affected by the presence of surface fluorides, we measured photocurrents collected on an inert Pt electrode immersed in pure TiO_2 or F−TiO_2 suspension in the presence of electron transfer mediators (electron shuttles) as illustrated in Scheme 1a. The collection of CB electrons using this method has been found to be efficient and convenient.[18,28,29] Methyl viologen redox couple (MV^{2+}/MV^+, $E° = -0.44$ V vs NHE) was used as an electron shuttle. The redox potential of this couple is pH-independent, whereas the potential of TiO_2 CB edge is pH-dependent (−59 mV shift per unit pH increased). Under this condition, the photocurrent collection mediated by the MV^{2+}/MV^+ couple is energetically not favored at acidic pH but is allowed at higher pH as illustrated in Scheme 1b.[29,30]

Figure 8a shows the time profiles of the methyl viologen mediated photocurrent generation in deaerated naked TiO_2 and F−TiO_2 suspensions at different pHs. The photocurrent is reduced at lower pH because the TiO_2 CB edge (E_{cb}) shifts to the positive with decreasing the potential difference between E_{cb} and $E°(MV^{2+}/MV^+)$. It is also noted that the photocurrent generated in the F−TiO_2 suspension is smaller than that in the pure TiO_2 suspension. This indicates that CB electron transfer

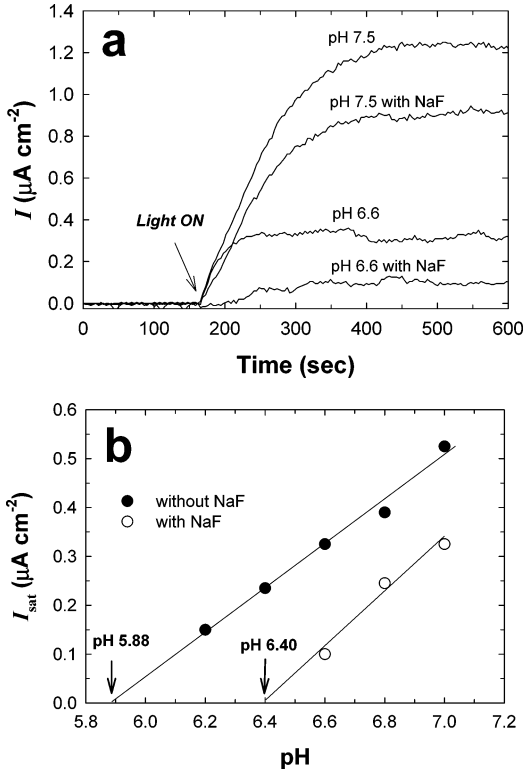

Figure 8. (a) Comparison of MV^{2+}-mediated photocurrent collected on a Pt electrode in deaerated TiO_2 suspensions with or without NaF. (b) Saturated photocurrent (I_{sat}) in (a) as a function of pH. Acetic acid was used as an electron donor. Experimental conditions: $[TiO_2] = 0.5$ g/L; $[NaF] = 10$ mM; $[MV^{2+}]_0 = 0.1$ mM; $[acetate]_0 = 20$ mM; Pt collector electrode held at +0.6 V vs SCE; continuously N_2-purged; illuminated with 30-W black light lamp.

to MV^{2+} is slower on F−TiO_2 than on naked TiO_2. This is consistent with the observation that TCA photoreduction is reduced on F−TiO_2. The plot of the saturated photocurrent (I_{sat}) as a function of pH (Figure 8b) shows different onset pHs (6.40 vs 5.88) between the F−TiO_2 and pure TiO_2 systems, which corresponds to the following onset potential difference (ΔE_{on}) in the CB electron transfer:

$$\Delta E_{on} = 59 \text{ mV/pH} \times (6.40 - 5.88) = 31 \text{ mV} \qquad (5)$$

This implies either that E_{cb}(F−TiO_2) is 31 mV positive of E_{cb}(naked TiO_2) or that CB electron transfer to MV^{2+} on F−TiO_2 needs a higher overpotential than on naked TiO_2. Considering the previous observation that the flat-band potential (E_{fb}) shifted to negative values upon fluoride adsorption on TiO_2 in acetonitrile,[11] the former hypothesis is not plausible. The latter assumption of a higher overpotential on F−TiO_2 sounds more reasonable.

Figure 9 compares the photocurrent collected in the suspension of TiO_2, F−TiO_2, Pt/TiO_2, and Pt/F−TiO_2 when using Fe^{3+} as an electron shuttle instead of MV^{2+}. Much higher photocurrents can be collected in this case, but it takes much longer time to reach a saturated current level with Fe^{3+} although the reduction potential of Fe^{3+} (0.77 V_{NHE}) is far more positive than that of MV^{2+} (−0.44 V_{NHE}). Adding NaF in the pure TiO_2 (or Pt/TiO_2) suspension reduces the Fe^{3+}-mediated photocurrent as in the case of Figure 8. As previously reported by this group,[18] the photocurrent collected in the Pt/TiO_2 suspension is higher than in the pure TiO_2 suspension since the platinization of TiO_2 surface enhances the rate of interfacial electron transfer by trapping CB electrons in the platinum phase and subsequently

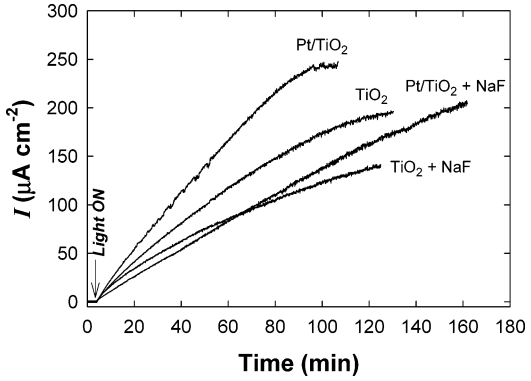

Figure 9. Comparison of Fe^{3+}-mediated photocurrent collected on a Pt electrode in deaerated suspensions of TiO_2, TiO_2 + NaF, Pt/TiO_2, and Pt/TiO_2 + NaF. Acetic acid was used as an electron donor. Experimental conditions: $[TiO_2] = [Pt/TiO_2] = 0.5$ g/L; $[NaF] = 10$ mM; $[Fe^{3+}] = 0.5$ mM; [acetate] = 0.2 M; $pH_i = 2.0$; other conditions identical to those of Figure 8.

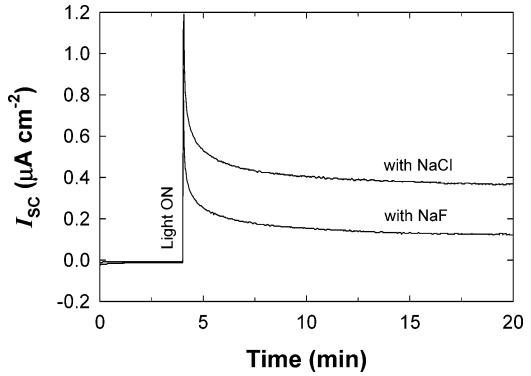

Figure 10. Time profiles of short-circuit photocurrent, I_{sc}, obtained with an illuminated TiO_2/Ti electrode in the presence of NaCl or NaF. Experimental conditions: [NaCl] = [NaF] = 10 mM; $pH_i = 3.7$; open to air; illuminated with 30-W black light lamp.

retarding the fast charge recombination.[31] The electrons trapped in the Pt phase are thought to be more mobile (and loosely bound) than electrons trapped at TiO_2 surface sites and should be easily transferred to electron acceptors. The fact that the photocurrent collection is reduced in the presence of F^- regardless of the kind of electron shuttles used (MV^{2+} or Fe^{3+}) implies that the electrons trapped at F−TiO_2 surface sites are less likely to be transferred to electron acceptors. This also concurs with the result of TCA photoreduction on F−TiO_2 (Figure 7).

One might argue that the inhibiting effect of fluorides on the photocurrent collection could be caused by the complex formation between F^- and the electron shuttles (MV^{2+} or Fe^{3+}). To rule out this effect, the profiles of short-circuit photocurrent (I_{sc}) generation on an illuminated TiO_2/Ti electrode in aqueous solution with NaCl or NaF are compared in Figure 10. I_{sc} in the NaF solution is markedly smaller than in the NaCl solution, which is consistent with the photocurrent collection behaviors observed in the suspensions (Figures 8 and 9). Judging from this evidence, it is proposed that the reduced photocurrent generation on F−TiO_2 (regardless of its physical forms: a suspended particle or an electrode) is due to the large electronegativity of surface fluoride species.

Charge Transfer Processes on F−TiO_2 and the Effect of Illumination on Surface Fluorination. Scheme 2 illustrates the elementary charge transfer processes occurring on naked TiO_2 and F−TiO_2. On F−TiO_2, the direct VB hole trapping is not allowed but the free OH radical formation is enhanced

SCHEME 2: Elementary Reaction Steps in the Photoinduced Charge Transfer and Fluorination Processes Occurring on Naked TiO_2 and F−TiO_2 under Both Dark and Illumination Conditions

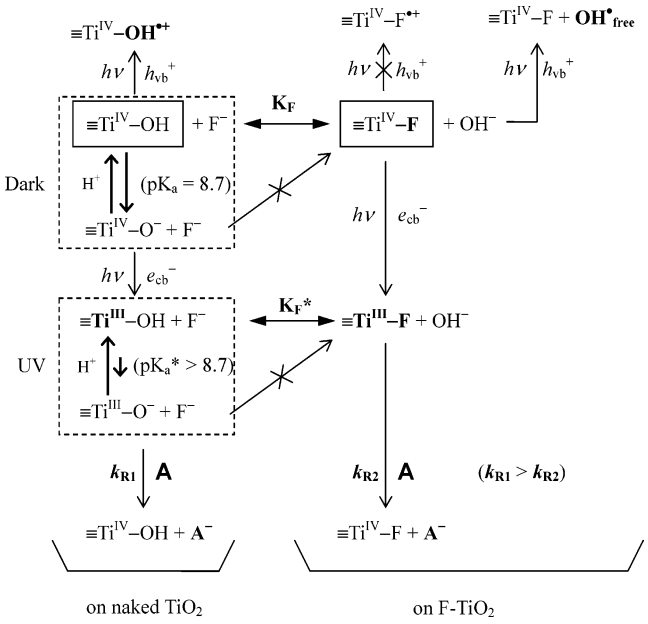

instead, mainly due to the surface coverage of ≡Ti−F species. The formation of surface-bound OH radicals seems to be favored only on naked TiO_2 surface. On the other hand, the CB electron trapping should be also affected by the presence of ≡Ti−F species. It is proposed that the electrons trapped at $\equiv Ti^{III}-F$ sites are more strongly bound than those at $\equiv Ti^{III}-OH$ sites due to the strong electronegativity of the fluorine. This might be similar to the proposal by Yu et al.[32] that trifluoroacetate (carrying a strongly electron withdrawing $-CF_3$ group) complexed on TiO_2 surface could trap CB electrons with reduction of the charge-pair recombination.

On the other hand, it should be recognized that the fluoride adsorption equilibrium in the dark could be perturbed by UV illumination (i.e., $K_F \neq K_F^*$). Under a photostationary state, the surface charge of suspended TiO_2 particles in water is shifted to the negative side due to the accumulation of trapped CB electrons.[33] Most trapped electrons are localized at $\equiv Ti^{III}-OH$ surface sites. In a previous infrared spectroscopic study,[34] it was found that the surface O−H stretching frequency is higher in $Ti^{III}O-H$ than in $Ti^{IV}O-H$ group by 69 cm^{-1}, which implies that $Ti^{III}O-H$ (generated under illumination) should be less acidic than $Ti^{IV}O-H$ group that has the pK_a value of 8.7 (Ti^{IV}-OH ↔ $Ti^{IV}O^- + H^+$).[14] Therefore, pK_a of $Ti^{III}O-H$ should be higher than 8.7. The different surface acidity constant under illumination may change the surface fluoride concentration under illumination. For example, at around pH 9 as illustrated in Scheme 2, the surface concentration ratio $[\equiv Ti^{III}-OH]/[Ti^{III}O^-]$ (under illumination) should be higher than $[\equiv Ti^{IV}-OH]/[Ti^{IV}O^-]$ (in the dark) and the surface fluorination reaction should be favored with ≡Ti−OH, not with $\equiv Ti-O^-$ group. As a result, more fluorides could be adsorbed on TiO_2 surface under illumination than in the dark. This might provide an explanation for why the photocatalytic degradation of phenol (or TCA) is enhanced (or inhibited) in the presence of F^- at basic pH where the dark equilibrium surface concentration of ≡Ti−F should be negligible (see Figures 5 and 7). If some ≡Ti−F species are formed even at pH 9 under illumination, enhanced photocatalytic oxidation through free OH radicals generation could be expected. As for the reduction part, the trapped electrons at the $\equiv Ti^{III}-F$ sites are more slowly abstracted by electron acceptors, A (e.g., TCA, MV^{2+}, Fe^{3+}), than those at the $\equiv Ti^{III}-OH$ sites; hence $k_{R1} > k_{R2}$.

Conclusions

The effects of TiO_2 surface fluorination on the photocatalytic and photoelectrochemical activity, some of which are the reconfirmation of previous studies[13,14] and others newly found in this study, can be summarized as follows. (1) The generation of free OH radicals is enhanced on F−TiO_2 because direct hole trapping or the generation of surface-bound OH radicals is not allowed on the fluorinated surface. (2) Substrates that react mainly through an OH radical mediated pathway are more rapidly degraded in the F−TiO_2 suspension, whereas substrates whose degradation is initiated by a direct hole transfer show slower kinetics due to their hindered adsorption (or complexation) on F−TiO_2. (3) Surface fluoride formation greatly lowers positive surface charges on TiO_2 at acidic pH region (pH < 6) and reduces the electrostatic interaction with charged substrates. (4) The surface ≡Ti−F group acts as an electron-trapping site but reduces interfacial electron transfer rates by tightly holding trapped electrons due to the strong electronegativity of the fluorine. As a result, both photoreductive dechlorination of TCA and the photocurrent generation are reduced on F−TiO_2. (5) The fluoride adsorption on illuminated TiO_2 surface might be enhanced from the dark equilibrium concentration. This may induce the generation of ≡Ti−F species even at alkaline pH. Although surface fluorination of TiO_2 can be attained by a simple addition of fluorides, it seems to significantly change interfacial charge transfer kinetics and affects photocatalytic and photoelectrochemical activities. Incidentally, comparing the photocatalytic degradation kinetics between the pure TiO_2 and F−TiO_2 systems provides valuable mechanistic information. For example, if the photocatalytic degradation rate of a specific substrate is little affected or reduced on F−TiO_2 (e.g., DCA case), this implies that the OH radical mediated path is less important. On the other hand, if F−TiO_2 increases the degradation rate (e.g., phenol, AO7 cases), the overall photocatalytic oxidation process on pure TiO_2 is probably limited by a fast charge recombination via adsorbed substrates.

Acknowledgment. This work was supported by KOSEF through the Center for Integrated Molecular Systems (CIMS) and partly by the Brain Korea 21 project.

References and Notes

(1) *Photocatalysis: Fundamentals and Applications*; Serpone, N., Pelizzetti, E., Eds.; John Wiley & Sons: New York, 1989.

(2) *Photocatalytic Purification and Treatment of Water and Air*; Ollis, D. F., Al-Ekabi, H., Eds.; Elsevier: Amsterdam, 1993.

(3) Hoffmann, M. R.; Martin, S. T.; Choi, W.; Bahnemann, D. W. *Chem. Rev.* **1995**, *95*, 69.

(4) Peral, J.; Domenech, X.; Ollis, D. F. *J. Chem. Technol. Biotechnol.* **1997**, *70*, 117.

(5) (a) Cho, S.; Choi, W. *J. Photochem. Photobiol. A* **2001**, *143*, 221. (b) Lee, M. C.; Choi, W. *J. Phys. Chem. B* **2002**, *106*, 11818. (c) Choi, W.; Hong, S. J.; Chang, Y.-S.; Cho, Y. *Environ. Sci. Technol.* **2000**, *34*, 4810. (d) Kim, S.; Choi, W. *Environ. Sci. Technol.* **2002**, *36*, 2019. (e) Lee, H.; Choi, W. *Environ. Sci. Technol.* **2002**, *36*, 3872. (f) Lee, J.; Park, H.; Choi, W. *Environ. Sci. Technol.* **2002**, *36*, 5462. (g) Bae, E.; Choi, W. *Environ. Sci. Technol.* **2003**, *37*, 147. (h) Choi, W.; Lee, J.; Kim, S.; Hwang, S.; Lee, M. C.; Lee, T. K. *J. Ind. Eng. Chem.* **2003**, *9*, 96.

(6) Kamat, P. V. *Chem. Rev.* **1993**, *93*, 267.

(7) Subbarao, S. N.; Yun, Y. H.; Kershaw, R.; Dwight, K.; Wold, A. *Inorg. Chem.* **1979**, *18*, 488.

(8) Hattori, A.; Yamamoto, M.; Tada, H.; Ito, S. *Chem. Lett.* **1998**, 707.

(9) Hattori, A.; Shimoda, K.; Tada, H.; Ito, S. *Langmuir* **1999**, *15*, 5422.

(10) Yu, J. C.; Yu, J.; Ho, W.; Jiang, Z.; Zhang, L. *Chem. Mater*. **2002**, *14*, 3808.
(11) Wang, C. M.; Mallouk, T. E. *J. Phys. Chem.* **1990**, *94*, 423.
(12) Wang, C. M.; Mallouk, T. E. *J. Phys. Chem.* **1990**, *94*, 4276.
(13) (a) Minero, C.; Mariella, G.; Maurino, V.; Pelizzetti, E. *Langmuir* **2000**, *16*, 2632. (b) Minero, C.; Mariella, G.; Maurino, V.; Vione, D.; Pelizzetti, E. *Langmuir* **2000**, *16*, 8964.
(14) Vohra, M. S.; Kim, S.; Choi, W. *J. Photochem. Photobiol. A* **2003**, *160*, 55.
(15) Lewandowski, M.; Ollis, D. F. *J. Catal.* **2003**, *217*, 38.
(16) Herrmann, M.; Kaluza, U.; Bohem, H. P. *Z. Anorg. Chem.* **1970**, *372*, 308.
(17) Wardman, P. *J. Phys. Chem. Ref. Data* **1989**, *18*, 1637.
(18) Park, H.; Choi, W. *J. Phys. Chem. B* **2003**, *107*, 3885.
(19) Rodríguez, R.; Blesa, M. A.; Regazzoni, A. E. *J. Colloid Interface Sci.* **1996**, *177*, 122.
(20) Dunn, W. W.; Aikawa Y.; Bard, A. J. *J. Am. Chem. Soc.* **1981**, *103*, 3456.
(21) Moser, J.; Punchihewa, S.; Infelta, P. P.; Grätzel, M. *Langmuir* **1991**, *7*, 3012.
(22) Choi, W.; Hoffmann, M. R. *Environ. Sci. Technol.* **1995**, *29*, 1646.
(23) Bauer, C.; Jacques, P.; Kalt, A. *J. Photochem. Photobiol. A* **2001**, *14*, 87.
(24) Vinodgopal, K.; Wynkoop, D. E.; Kamat, P. V. *Environ. Sci. Technol.* **1996**, *30*, 1660.
(25) Cho, Y.; Choi, W. *J. Photochem. Photobiol. A* **2002**, *148*, 129.
(26) Bahnemann, D. W.; Kholuiskaya, S. N.; Dillert, R.; Kulak, A. I.; Kokorin, A. I. *Appl. Catal. B* **2002**, *36*, 161.
(27) Kim, S.; Choi, W. *J. Phys. Chem. B* **2002**, *106*, 13311.
(28) Ward, M. D.; Bard, J. A. *J. Phys. Chem.* **1982**, *86*, 3599.
(29) Ward, M. D.; White, J. R.; Bard, A. J. *J. Am. Chem. Soc.* **1983**, *105*, 27.
(30) Duonghong, D.; Ramsden, J.; Grätzel, M. *J. Am. Chem. Soc.* **1982**, *104*, 2977.
(31) Kamat, P. V. *J. Phys. Chem. B* **2002**, *106*, 7729.
(32) Yu, J. C.; Ho, W.; Yu, J.; Hark, S. K.; Iu, K. *Langmuir* **2003**, *19*, 3889.
(33) Dunn, W. W.; Aikawa, Y.; Bard, A. J. *J. Am. Chem. Soc.* **1981**, *103*, 3456.
(34) Szczepankiewicz, S. H.; Moss, J. A.; Hoffmann, M. R. *J. Phys. Chem. B* **2002**, *106*, 7654.